Tire Rubber–Sisal Composites: Effect of Mercerization and Acetylation on Reinforcement

Maria Alice Martins, Ines Joekes

Instituto de Química, Universidade Estadual de Campinas, UNICAMP, C.P. 6154, CEP 13084-971, Campinas, SP, Brazil

Received 1 April 2002; accepted 16 October 2002

ABSTRACT: Tire rubber particles were mixed randomly with short sisal fibers and hot pressed. Sisal fibers were used as received, mercerized, and mercerized/acetylated. The fibers were characterized by scanning electron microscopy (SEM), thermal gravimetry analysis (TGA), infrared spectroscopy (FTIR), water sorption, and mechanical properties. Thermal stability of the mercerized/acetylated fibers improves (from 200 to 300°C) with respect to the raw fibers, and water sorption is ~ 20% smaller than for the raw and the mercerized fibers. Tensile strength is unchanged after the chemical treatments. Water sorption, mechanical properties, and SEM evaluated the performance of the tire rubber composites. All composites showed enhanced elastic modulus; increase is dependent on fiber load. Smallest water sorption was obtained in composites with the mercerized/acetylated fibers. With these fibers at 10% load, the best results were obtained with the smaller tire rubber particles (320 μm) and at 5% load with the bigger (740 μm) tire rubber particles. Both composites showed ~ 50% increase in tensile strength when compared to similar composites with raw fibers. SEM of the surface of fracture showed that the adhesion between fiber and rubber was enhanced after both chemical treatments. J Appl Polym Sci 89: 2507–2515, 2003

Key words: sisal fibers; renewable resources; tire rubber; composites; fiber modification

INTRODUCTION

Elastomer composites reinforced with fibers are an ever-growing class of materials because of their improved physical and mechanical properties, plain processability, and economic advances. These materials combine the stiffness of fibers with the elasticity of rubber.[1–3] Shifting from synthetic fibers and polymers to natural fibers and recycled polymers renders environmentally friendly materials. In developing countries, natural fiber crops are also important to generate jobs that improve social and economical conditions. However, very few articles report on natural fiber-recycled polymer composites. The aim of this work was to obtain and characterize composites from Brazilian sisal fibers and tire rubber particles.

Sisal fiber is one of the most widely used natural fibers and is very easily cultivated. Almost 4.5 million tons of sisal fibers are produced every year throughout the world.[4] Brazil is the biggest producer and the Brazilian Agricultural Research Corp. (Embrapa) is studying new varieties of sisal for the Northeast region of the country to improve yield and fiber properties.[5] Sisal is a hard fiber extracted from the leaves of the plant. A sisal plant produces roughly 200–250 leaves, each containing 1000–1200 fiber bundles composed of 4% fiber, 0.75% cuticle, 8% dry matter, and 87.25% water.[5,6] The sisal leaf contains three types of fibers: mechanical, ribbon, and xylem.[4,7,8]

The properties of natural fiber–elastomer composites depend on those of the individual components and on their interfacial compatibility.[4] Strong adhesion at the fiber–matrix interface is crucial for the use of natural fibers as reinforcements in polymers and elastomers. Physical and chemical methods are used to maximize this adhesion.[9,10] Several studies by Thomas and coworkers, on the properties of short sisal fiber-reinforced natural rubber[11–13] and styrene butadiene rubber[14–16] composites, show that chemically treated fibers render mechanical and viscoelastic improved composites, which also depend on the fiber orientation and fiber length. Fiber lengths of 10 mm (for natural rubber) and 6 mm (for styrene butadiene) were found to confer the best balance of properties.

The manufacture of products from recycled materials has technologic, economic, and environmental advantages that have become attractive in recent years.[17] The growing amount of waste rubber, produced from tires, has resulted in a serious environmental problem. In Brazil, about 32 million tires are produced annually and it is estimated that 10 to 15 million units are discarded each year.[18] Only a fraction of the scrap tire

Correspondence to: I. Joekes (ines@iqm.unicamp.br).
Contract grant sponsor: FAPESP; contract grant number: 00/14760-7.

Journal of Applied Polymer Science, Vol. 89, 2507–2515 (2003)

in Brazil and in the world is recycled,[18,19] although efforts have been made to increase their uses.

Very few works have been reported on the reuse of tire rubber in composites. Song et al.[17,20] studied composites of wood fibers and tire rubber crumbs, with up to 20% amounts of diphenylmethane diisocyanate (MDI) resin. Good adhesion was found by using compression molding.

In this work, the performance of tire rubber composites with Brazilian sisal fibers was studied. The effect of chemical modification (mercerization and acetylation) of the fibers on the composite performance was followed by water sorption, mechanical properties, and scanning electron microscopy (SEM).

EXPERIMENTAL

Materials

The samples of sisal fibers used in this work are from the variety *Agave sisalana*. Samples belong to the first year of harvest, after processing. This process includes fiber separation from the leaves, washing, drying, combing, and baling. The samples used in this work are those wasted in the last two steps. The density of the fibers was measured in a Micromeritics 1305 helium pycnometer as 1.26 ± 0.03 g/cm^3. The diameter was measured on 100 fibers by using a Mitutoyo micrometer as 114 ± 40 μm. Martin[21] studied the composition and structure from 14 varieties of sisal fibers studied by Embrapa. The results for (cyclohexane/ethanol extracted, water rinsed, dried) *A. sisalana* are as follows: cellulose: 75.2 ± 0.3%; hemicellulose: 13.87 ± 0.09%; lignin: 7.98 ± 0.05%; ash: 0.87 ± 0.01%.

Borcol Indústria de Borracha Ltd. (Sorocaba/S.P., Brazil) supplied the samples of powdered tire rubber (from bus and truck tires) with 320 and 740 μm average particle size. The processing steps to obtain these particles are as follows: after removing the tread of the tires, the resulting scrap is ground in a series of knife mills, where cyclone and suck pumping separate metal particles and synthetic fibers. Mills have an outflow-sieving device to control the final particle size. Particles are mainly composed of natural rubber and styrene butadiene rubber, as shown by infrared analysis, and have a density of 1.152 ± 0.001 g cm^{-3}.[18] The particles are unsuitable for the Mooney viscosity test and have an average sol/gel ratio of 0.16 ± 0.01 before processing and of 0.20 ± 0.03 after processing; the same values were obtained after 1, 2, and 3 days extraction in toluene.

Sodium hydroxide (NaOH), sulfuric acid (H_2SO_4), glacial acetic acid, and acetic anhydride analytical grade reagents were used.

Methods

Fifty-gram samples of raw sisal fibers were washed in distilled water at 80 ± 2°C for 1 h, mercerized with NaOH 5 or 10%, at room temperature (26 ± 2°C), 50 or 80°C, for 1, 3, or 5 h, rinsed with tap water, neutralized with acetic acid, and dried in a microwave oven for 15 min. The mass loss was measured after washing and mercerizing.

For acetylation, 50-g samples of raw or mercerized fibers were immersed in glacial acetic acid for 1 h at room temperature (26 ± 2°C) and then immersed in 500 mL of acetic anhydride containing 20 drops of concentrated sulfuric acid for 5 min.[22] The fibers were separated in a Buchner funnel, rinsed with tap water until pH 6 to 7, and dried in a microwave oven for 15 min. The average weight increase after acetylation was 2% for the mercerized fibers. The infrared spectra of the acetylated sisal fibers show absorption peaks at 1740 cm^{-1} (ester C═O), at 1375 cm^{-1} (νC—CH$_3$), and at 1235 cm^{-1} (νC—O), which provide evidence of successful acetylation.[12,23,24]

Composites containing 5, 10, 20, and 30 wt % of raw, mercerized, and mercerized/acetylated fibers were prepared by using both tire rubber samples. The raw and treated sisal fibers were chopped using a knife mill. The length distributions showed that ~ 70% of sisal fibers were 1.6 mm. The chopped fibers and the rubber particles were mixed by hand in the proper amounts. Randomly oriented (160 × 150 × 3 mm) composite sheets were prepared by hot-press molding at 10.000 kgf, 200°C, for 3 h. These hot-press conditions were previously established.[25]

Infrared spectra of treated and raw sisal fibers were recorded on a Bomem Hartmann and Braun B100-MB spectrophotometer, in KBr pellets. FTIR-multiple internal reflection (MIR) spectra were recorded on a Nicolet Magna FTIR 550 spectrophotometer. Thermogravimetric analysis (TGA) and differential thermogravimetry (DTG) were obtained in a TA Instruments 5100-TGA 2050, in the temperature range of 25 to 800°C, at a heating rate of 3°/min in an argon atmosphere.

Water sorption of the fibers was measured by immersing 1 g of the sisal fibers in tap water at room temperature. After removal, surfaces were dried without squeezing between paper towels. Mass increase with respect to the initial dry mass was measured as a function of time. Water sorption of the composites was measured by immersing samples in tap water at room temperature, following ASTM D 570-95.[26]

Tensile measurements of the fibers followed ASTM D 3379-75.[27] The individual fibers were fixed to a cardboard window, 5 cm long. At least 50 filaments were conditioned at 20 ± 2°C and 50 ± 5% relative humidity for no less than 48 h before testing on an EMIC DL 2000 Universal Testing Machine, at a speed of 2 mm/min. Measurements of the mechanical properties of the composites followed ASTM D 412-92,[28] at a speed of 10 mm/min. The samples were conditioned at 20 ± 2°C and 50 ± 5% relative humidity for at least 48 h before testing.

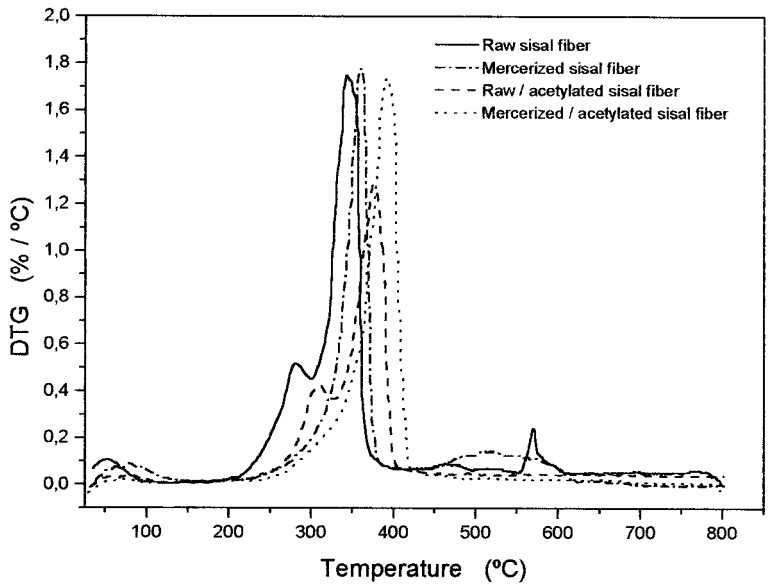

Figure 1 Differential thermogravimetic analysis (DTG) of raw and treated sisal fibers. Temperature range 25–800 °C, 3 degree/min. Argon atmosphere. Duplicate results are coincident.

For the analysis of fracture surfaces of the sisal fibers and of the composites, the samples were immersed in liquid nitrogen for 15 min and fractured. For SEM, the samples were glued in proper stubs and covered with gold in a Sputter Edward S 150 B and observed in a JEOL JSM 840 A, operating at 25 kV.

RESULTS AND DISCUSSION

Sisal fibers

Mercerization is an alkali treatment of cellulose fibers that depends on the type and concentration of the alkaline solution, temperature, and time of treatment.[10] Results obtained for the sisal fibers after the mercerization treatment showed that mass loss depends more on temperature than on time. The mercerization treatment leads to an average mass loss of 22 ± 3% (w/w) for NaOH 5%, and of 27 ± 5% (w/w) for NaOH 10%. Infrared and MIR-infrared results show that lignin and hemicellulose were removed from the surface and the interior of the fibers. The mass loss takes account, also, of the removal of soluble matter during washing.

Figures 1 and 2 show DTG and TGA profiles of raw, mercerized, raw-acetylated, and mercerized/acetylated sisal fibers. The DTG curves show an initial peak

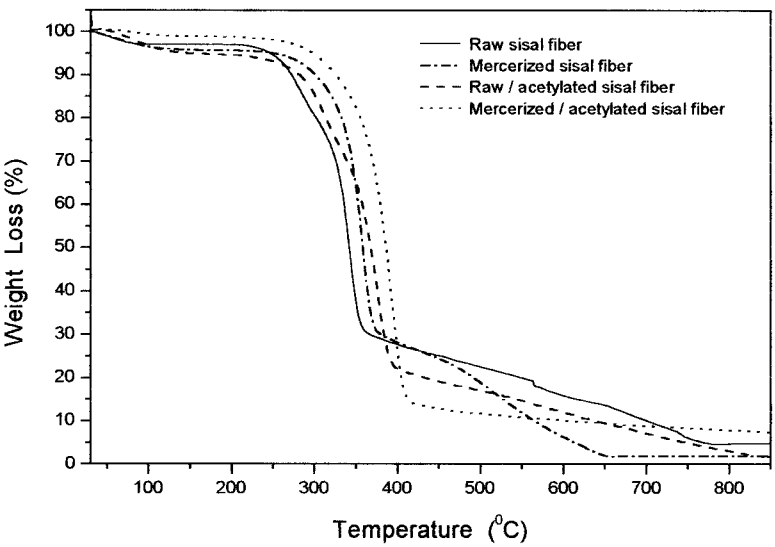

Figure 2 Thermogravimetric analysis (TGA) of raw and treated sisal fibers. Temperature range 25–800 °C, 3 degree/min. Argon atmosphere. Duplicate results are coincident.

TABLE I
Mechanical Properties of the Sisal Fibers (ASTM D 33379-75)

Fiber	Modulus (10 GPa)	Elongation at break (%)	Tensile strength (GPa)
Raw	5 ± 2	4 ± 2	1.3 ± 0.6
Mercerized (5% NaOH, 5 h, 80°C)	5 ± 2	3 ± 1	1.1 ± 0.5
Mercerized (10% NaOH, 5 h, 80°C)	5 ± 2	3 ± 1	1.1 ± 0.4
Mercerized (5% NaOH, 5 h, 80°C) and acetylated	4 ± 2	3 ± 1	1.0 ± 0.4

between 50 and 100°C, which corresponds to water loss in the all samples. After this peak, the DTG curve of the raw fibers show three decomposition steps: (1) the first decomposition peak at about 280°C is attributed to thermal depolymerization of hemicellulose and the glycosidic linkages of cellulose; (2) the second decomposition peak at about 340°C is attributed to α-cellulose decomposition (weight loss ~ 70%); (3) the small peak at 570°C (weight loss ~ 20%) may be attributed to oxidative degradation of the charred residue. The thermograms show an improvement in the thermal stability of the modified fibers in relation to the raw fiber. The main decomposition temperature increases from 340°C (raw) to 350°C for the mercerized fibers and to 395°C for the mercerized/acetylated fibers. There is a change in the degradation mechanism: in the mercerized/acetylated fibers there is only one stage, and in the mercerized fibers and in the raw/acetylated fiber there are two, whereas for the raw fibers there are three. In the acetylated sisal fiber the peak due to oxidative degradation of the charred residue is missing, which indicates that the acetylated material is lost as volatile products and does not contribute to char formation. These observations agree with the literature.[29–31]

Mechanical properties of raw and treated fibers are shown in Table I. There is no significant variation in tensile strength, elongation at break, and Young's modulus after the treatments, indicating that there is no significant damage in the structure of the fibers.

The amount of water sorbed by the fibers is shown in Figure 3. The raw and the mercerized fibers sorb a maximum of ~ 80% of their weight in the first minute. No difference was observed for fibers mercerized in different conditions. Water sorption by the mercerized/acetylated fibers is ~ 20% smaller than for the mercerized and raw fibers.

Figure 4 shows characteristic SEM micrographs of raw and treated fibers. Figure 4(A) shows the surface structure of the raw fibers. The fiber surface is marked by the characteristic vestigial attach of the parenchymatous cells in which the fiber was embedded in the leaf. The surface of the mercerized fiber in Figure 4(B) is quite changed, showing the partial loss of the parenchyma cells, the removal of the impurities and waxy cuticle layers on the fiber surface, and an incipient defibrillation due to the extraction of the hemicellulose and the cementing components, such as lignin. This increases the effective surface area available of contact with the matrix. Figure 4(C) shows a mercerized/acetylated fiber in which the coating with cellulose acetate due to heavy incorporation of acetyl group in the fibrils is evidenced.

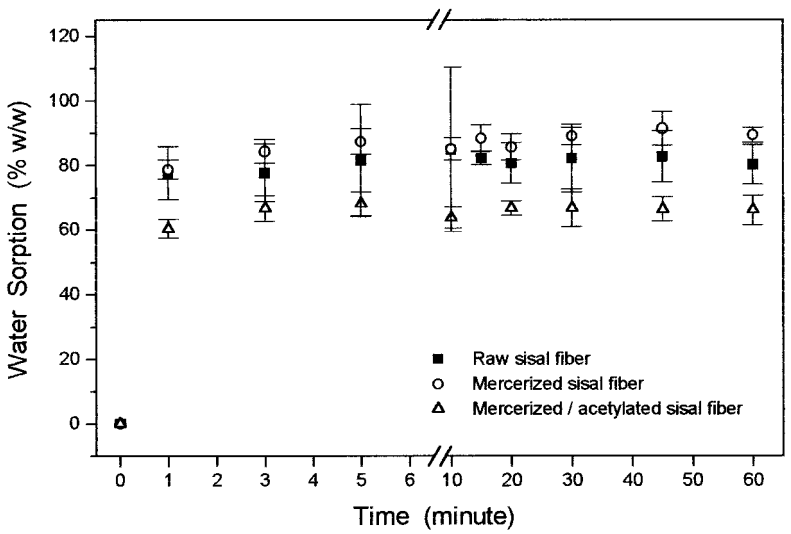

Figure 3 Percent increase in weight after tap water sorption, as a function of time of immersion, for raw and treated sisal fibers. Triplicate results. Room temperature.

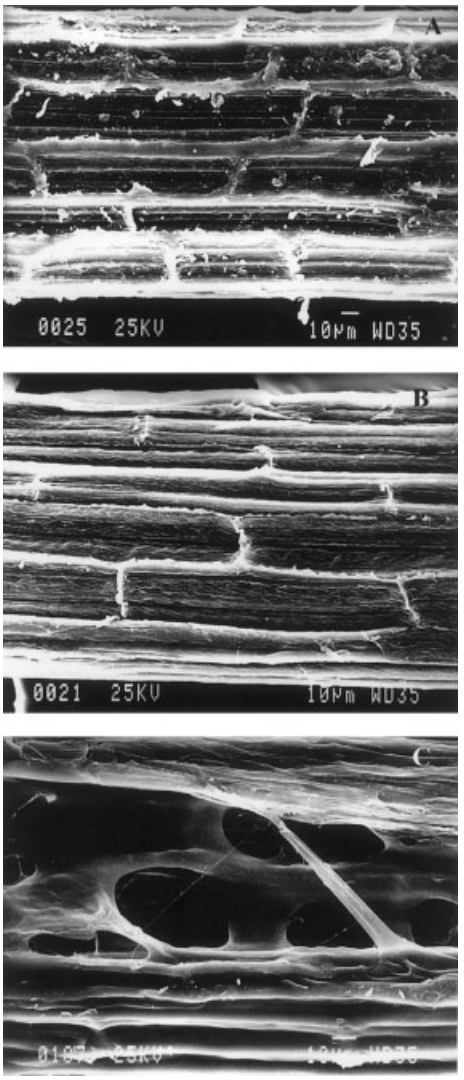

Figure 4 Scanning electron micrographs of sisal fibers: raw (A); mercerized (NaOH 5%, 80 °C, 5 h) (B); and mercerized (NaOH 5%, 80 °C, 5 h)/acetylated (C).

Composites

Mechanical properties measured for the composites based on tire rubber particles (320 and 740 μm average particle) and raw or treated sisal fibers are shown in Tables II and III. Young's modulus increases with increasing fiber load in all cases, as expected. Tensile strength and elongation decrease in all but a few cases compared to the matrix without fibers.

In the composites obtained with the smaller particles, the treated fibers render higher modulus than the raw fibers, at the same loading. Also, a maximum in tensile strength is obtained at 10% loading for mercerized/acetylated fibers and at 30% loading for mercerized fibers. The 30% loaded composite has a small elongation value and is stiffer. In this way, the best composite is obtained with the mercerized/acetylated fibers at 10% load, which shows $\sim$ 50% increase in tension strength and elongation (in relation to the raw fibers). Only in this case, the expected response to fiber loading is observed, namely, at low fiber loading, the matrix dominates the tensile strength and the fibers act as network defects[32–33]; increasing fiber load (up to 10%) gives a maximum in the tensile strength. At higher fiber loading, poor dispersion of the fibers in the tire rubber matrix was observed, leading to a decrease in performance.

In the composites obtained with the bigger particles, no significant correlation is observed between fiber treatment and modulus. The best strength and elongation performance ($\sim$ 50% increase in relation to the raw fibers) is observed with the mercerized/acetylated fibers at the lowest loading, 5%. Because no data were obtained for loadings smaller than 5%, it is not possible to associate this increased performance with the expected optimal loading.

Figures 5 and 6 show the water sorption data for the composites. The amount of water sorbed is related to the porosity of the specimens and gives a picture of their internal microstructure.[18] The matrices obtained

TABLE II
Mechanical Properties of the Small-Particle Tire Rubber Composites (ASTM D 412-92)

Property	Fiber	Load (%) 0	5	10	20	30
Young's modulus (MPa)	(Tire rubber)	5.2 ± 0.3	—	—	—	—
	Raw	—	6.8 ± 0.7	8 ± 1	14 ± 2	19 ± 3
	Mercerized	—	7.9 ± 0.5	11.4 ± 0.8	21 ± 8	36 ± 5
	Mercerized/acetylated	—	9 ± 1	12 ± 2	17 ± 4	28 ± 7
Tension strength at maximum force (MPa)	(Tire rubber)	1.3 ± 0.1	—	—	—	—
	Raw	—	1.1 ± 0.2	1.1 ± 0.1	1.0 ± 0.1	0.9 ± 0.1
	Mercerized	—	1.2 ± 0.1	1.2 ± 0.1	1.4 ± 0.2	1.6 ± 0.2
	Mercerized/acetylated	—	1.1 ± 0.1	1.7 ± 0.1	1.2 ± 0.1	1.2 ± 0.1
Elongation at maximum force (%)	(Tire rubber)	50 ± 5	—	—	—	—
	Raw	—	36 ± 4	39 ± 3	26 ± 7	18 ± 3
	Mercerized	—	42 ± 3	30 ± 2	15 ± 3	10 ± 1
	Mercerized/acetylated	—	34 ± 3	57 ± 3	33 ± 7	17 ± 4

TABLE III
Mechanical Properties of the Big-Particle Tire Rubber Composites (ASTM D 412-92)

Property	Fiber	Load (%) 0	5	10	20	30
Young's modulus (MPa)	(Tire rubber)	6.0 ± 0.4	—	—	—	—
	Raw	—	10 ± 2	10 ± 1	17 ± 3	27 ± 7
	Mercerized	—	7 ± 1	10 ± 1	18 ± 3	37 ± 17
	Mercerized/acetylated	—	6.6 ± 0.3	10 ± 1	17 ± 5	26 ± 12
Tension strength at maximum force (MPa)	(Tire rubber)	1.2 ± 0.2	—	—	—	—
	Raw	—	1.0 ± 0.1	1.1 ± 0.1	0.9 ± 0.2	0.7 ± 0.2
	Mercerized	—	1.0 ± 0.1	1.0 ± 0.1	1.1 ± 0.1	1.2 ± 0.3
	Mercerized/acetylated	—	1.5 ± 0.1	1.0 ± 0.1	1.0 ± 0.1	0.6 ± 0.2
Elongation at maximum force (%)	(Tire rubber)	60 ± 13	—	—	—	—
	Raw	—	35 ± 9	45 ± 5	22 ± 3	9 ± 3
	Mercerized	—	43 ± 4	39 ± 6	24 ± 4	9 ± 2
	Mercerized/acetylated	—	71 ± 5	36 ± 4	23 ± 4	6 ± 1

with the bigger particles sorb ~ 50% less water than the matrices with the smaller particles, indicating that they are less porous. As expected, the addition of sisal fibers to the rubber increases the water sorption, because the fibers are hydrophilic and porous. Also, the amount of water sorbed increases with loading. However, the saturation value is smaller than that calculated from a linear correlation with (wetted) fiber mass.

Mercerization removes a large quantity of lignin and hemicellulose, but roughness and microporosity of the fibers are greatly increased. This should improve mechanical anchorage and interlocking of the matrix with the mercerized fibers. This could explain the sorption behavior of the (less porous) bigger particle rubber composites, for which water sorption is lower than that of the composites with the raw fibers. However, water sorption in the (more porous) small-particle rubber composites is similar for both the mercerized and the raw fibers. In every case, water sorption by the composites with mercerized/acetylated fibers is less than all the others.

The composites that showed the best mechanical performance were those that sorbed less water: (1) the 10% mercerized/acetylated fibers composites show a decrease in water sorption of ~ 30% in the small-particle rubber matrix; and (2) the 5% mercerized/acetylated fibers composite show a decrease of ~ 50% in the big-particle rubber matrix, in relation to the raw fiber composites.

A SEM micrograph of the rubber particles is shown in Figure 7. The particles have a rough surface, with irregular shape and different sizes. Small particles appear aggregated on the bigger ones.

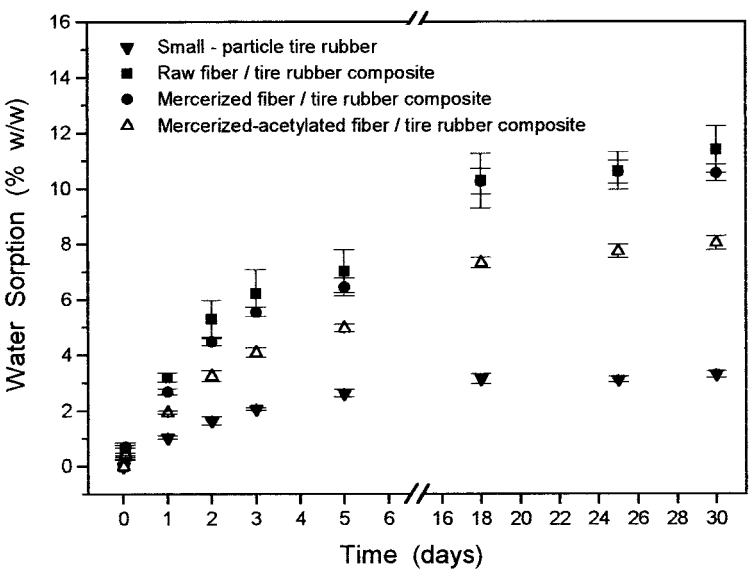

Figure 5 Percent increase in weight after tap water sorption, as a function of time of immersion, for small-particle tire rubber composites with raw and treated sisal fibers. Triplicate results. 10% fiber load. Room temperature.

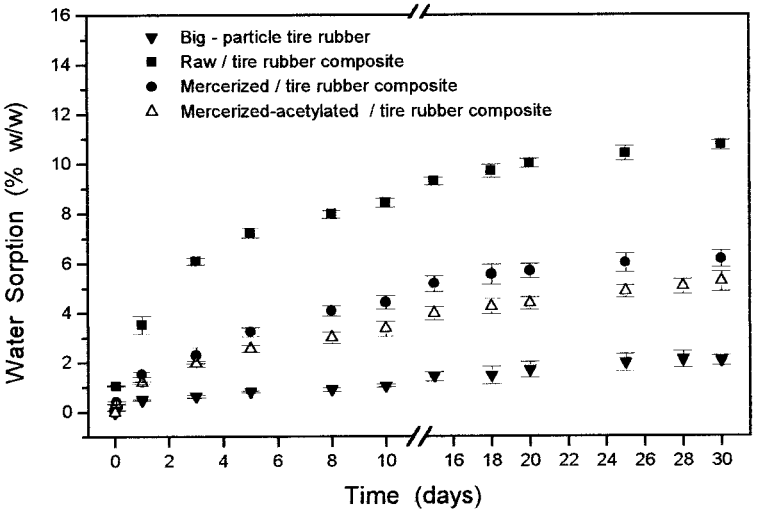

Figure 6 Percent increase in weight after tap water sorption, as a function of time of immersion, for big-particle tire rubber composites with raw and treated sisal fibers. Triplicate results. 5% fiber load. Room temperature.

The SEM micrograph in Figure 8 shows a typical fracture surface of a 10% fiber composite. The label (F) points to a sisal fiber dispersed in the rubber matrix (M). The label (A) shows a hole developed on the fracture surface due to the pullout of a sisal fiber. The arrow shows nylon filaments existing in the tire rubber particles, from the tire overlay. Poor adhesion can be observed between the nylon filaments and the sisal fibers with the rubber matrix, causing imperfections in the composite internal structure; this was observed for all fractures.

Figure 9 shows a SEM micrograph of the fracture surface of a 10% raw fiber composite, in which the weak interfacial adhesion is clear. Figure 10 shows the fracture surface of a 10% mercerized fiber composite showing no pull-out, which means that the cohesion energy of the rubber is lower than the fiber/matrix adhesion energy in the region of breaking. Figure 11 makes visible a strong adhesive joint between the shown mercerized/acetylated fiber and the rubber matrix. Cracking was lowest in the specimens of this type examined by SEM. No cracking means that the fracturing load was efficiently transferred from the matrix interface to the fibers, giving rise to an on-the-plane fiber breakage, as the one shown in this figure.

The effect of fiber content on fiber dispersion in the composite matrices was also observed by SEM. Good dispersion was observed in 5 and 10% raw or treated fiber composites. In composites with 20 or 30% fiber content, fiber/fiber interfaces were formed and led to poor interfacial adhesion.

The important data about the composites can be summarized as follows. FTIR-MIR results showed that the surface of the raw fibers has lignin and hemicellulose, and that both were almost removed

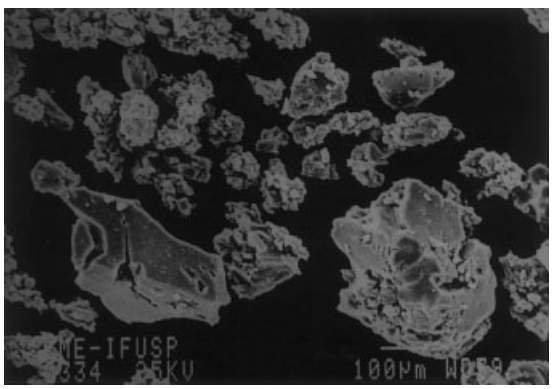

Figure 7 Scanning electron micrograph of the small particles of the tire rubber.

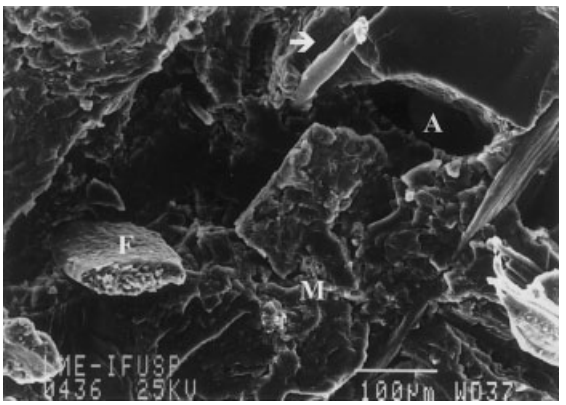

Figure 8 Scanning electron micrograph of a typical surface of fracture (liquid nitrogen) of mercerized sisal fiber reinforced (10% weight) small-particle tire rubber composite. M = rubber matrix, F = sisal fiber, A = hole on the surface due to pullout of a fiber. The arrow shows a nylon filament present in the tire rubber particles.

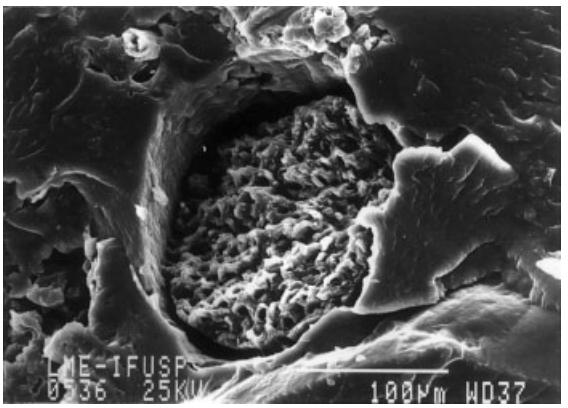

Figure 9 Scanning electron micrograph of a surface of fracture (liquid nitrogen) of raw sisal fiber reinforced (10% weight) small-particle tire rubber composite.

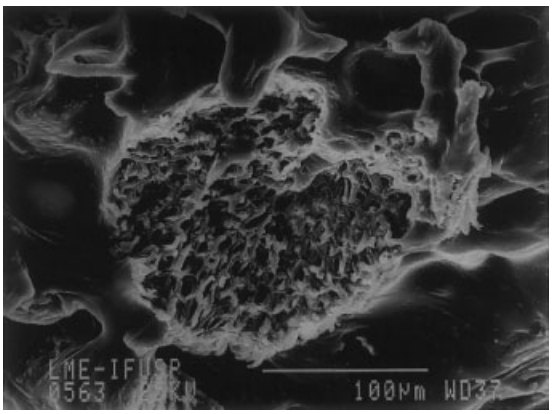

Figure 11 Scanning electron micrograph of a surface of fracture (liquid nitrogen) of a tire rubber composite (small particles) reinforced with mercerized/acetylated sisal fibers (10% weight).

after mercerization; also, that acetylation was more efficient on the mercerized than on the raw fibers. Mechanical tests showed that the composites obtained with the fibers have higher modulus, as expected. The best modulus values are obtained for the mercerized fibers. The best overall mechanical performance is obtained with the mercerized/acetylated fibers. Water sorption performance of the composites roughly follows the trend of the mechanical performance. SEM results showed that the surface (effective) area of the fibers increases from raw to mercerized/acetylated to mercerized. SEM also showed increasing strength in the adhesive joints from the raw to the mercerized to the mercerized/acetylated fiber composites. The tire rubber particles will adhere to the surface of the fibers, which increases and is less hydrophobic after lignin removal. Contact angles measured by Segre et al.[34] showed that the tire rubber particles have a significant number of polar groups. It is well known that adhesion improves as the number of van der Waals interactions increase. In this way, increased surface (effective) area and surface hydrophilic character explain the increased adhesion of the treated fibers.

CONCLUSION

Results show that the reuse of tire rubber in composites with sisal fibers is a new possibility for the application of these materials. Composite performance can be enhanced by chemically treating the sisal fibers. SEM shows better adhesive joints between the treated sisal fibers and the tire rubber. Values obtained for mechanical properties and water sorption and surface morphology show no significant difference for composites obtained with rubber particles of different average particle sizes. However, the best fiber loading was found to be 5 and 10%, depending on the tire rubber particle size.

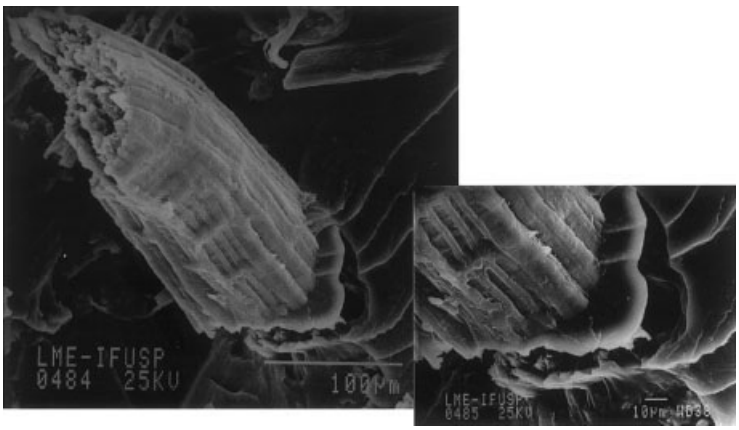

Figure 10 Scanning electron micrograph of a surface of fracture (liquid nitrogen) of mercerized sisal fiber reinforced (10% weight) small-particle tire rubber composite.

The authors thank LME-IF/USP for providing facilities to use the scanning electron microscope, Embrapa/CNPDIA for the supply of the sisal fibers, Borcol Ind. for the supply of the tire rubber and CNPq, and FAPESP (00/14760-7) for financial support.

References

1. Ismail, H.; Rosnah, N.; Rozman, H. D. Eur Polym J 1997, 33, 1231.
2. Geethamma, V. G.; Reethamma, J.; Thomas, S. J Appl Polym Sci 1995, 55, 583.
3. Nunes, R. C. R.; Visconte, L. L. Y. in Natural Polymers and Agrofibers Based Composites; Frollini, E.; Leão, A. L.; Mattoso, L. H. C., Eds.; USP, UNESP, and Embrapa: São Paulo, Brazil, 2000.
4. Li, Y.; Mai, Y.; Ye, L. Comp Sci Technol 2000, 60, 2037.
5. Mattoso, L. H. C.; Ferreira, F. C.; Curvelo, A. A. S. in Lignocellulose-Plastic Composites; Leão, A. L.; Carvalho, F. X.; Frollini, E., Eds.; USP and UNESP: São Paulo, Brazil, 1997.
6. Mukherjee, P. S.; Satyanarayana, K. G. J Mater Sci 1984, 19, 3925.
7. Nutman, F. J. Emp J Exp Agric 1936, 5, 75.
8. Medina, J. C.; Sisal, O. Secretaria da Agricultura do Estado de São Paulo: São Paulo, Brazil, 1954.
9. Bledzki, A. K.; Gassan, J. Prog Polym Sci 1999, 21, 221.
10. Mwaikambo, L. Y.; Ansell, M. P. Angew Makromol Chem 1999, 272, 108.
11. Varghese, S.; Kurialose, B.; Thomas, S. J Appl Polym Sci 1994, 53, 1051.
12. Varghese, S.; Kuriakose, B.; Thomas, S.; Koshy, A. T. J Adhes Sci Tech 1994, 8, 235.
13. Varghese, S.; Kuriakose, B.; Thomas, S. Polym Degrad Stab 1994, 44, 55.
14. Kumar, R. P.; Amma, M. L. G.; Thomas, S. J Appl Polym Sci 1995, 58, 597.
15. Kumar, R. P.; Thomas, S. Polym Int 1995, 38, 173.
16. Kumar, R. P.; Thomas, S. Sci Eng Compos Mater 1999, 8, 311.
17. Song, X. M.; Hwang, J. Wood Fiber Sci 1997, 29, 131.
18. Segre, N.; Joekes, I. Cem Concr Res 2000, 30, 1421.
19. Adhikari, B.; De, D.; Maiti, S. Prog Polym Sci 2000, 25, 909.
20. Song, X. M.; Hwang, M. Forest Prod J 2001, 51, 45.
21. Martin, A. R. Caracterização e Modificação de Fibras de Sisal Visando Aplicação em Compósitos Poliméricos, PhD Thesis, Univ. Federal de São Carlos, Brazil, 2001.
22. Chand, N.; Verma, S.; Khazanchi, A. C. J Mater Sci Lett 1989, 8, 1307.
23. Frisoni, G.; Baiardo, M.; Scandola, M. Biomacromolecules 2001, 2, 476.
24. Samal, R. K.; Panda, B. B.; Rout, S. K.; Mohanty, M. J Appl Polym Sci 1995, 58, 745.
25. Martins, M. A. Fibra de Sisal: Mercerização, Acetilação e Aplicação em Compósitos de Borracha de Pneu Triturado; PhD Thesis, Univ. Estadual de Campinas, Brazil, 2001.
26. ASTM D 570-95: Standard Test Method for Water Absorption of Plastics.
27. ASTM D 3379-75 (reapproved 1989): Standard Test Method for Tensile Strength and Young's Modulus for High-Modulus Single-Filament Materials.
28. ASTM D 412-92: Standard Test Method for Vulcanized Rubber and Thermoplastic Rubbers and Thermoplastic Elastomers—Tension.
29. Sabaa, M. W. Polym Degrad Stabil 1991, 32, 209.
30. Albano, C.; González, J.; Ichazo, M.; Kaiser, D. Polym Degrad Stab 1999, 66, 179.
31. Chand, N.; Sood, S.; Singh, D. K.; Rohatgi, P. K. J Therm Anal 1987, 32, 595.
32. Termonia, Y. J Polym Sci, Part B: Polym Phys 1994, 32, 969.
33. Termonia, Y. J Mater Sci 1990, 25, 4544.
34. Segre, N.; Monteiro, P. J. M.; Sposito, G. J Colloid Interface Sci 2002, 248, 521.